Elastic electron scattering in krypton in the energy range from 5 to 10 eV

Ireneusz Linert,[1] Brygida Mielewska,[1] George C. King,[2] and Mariusz Zubek[1]

[1]*Department of Physics of Electronic Phenomena, Gdańsk University of Technology, 80-233 Gdańsk, Poland*
[2]*School of Physics and Astronomy, Manchester University, Manchester M13 9 PL, United Kingdom*
(Received 18 November 2009; published 22 January 2010)

Differential cross sections for elastic electron scattering in krypton have been measured at the energies of 5, 7.5, and 10 eV over the scattering angle range from 30° to 180°. The measurements for backward scattering employed the magnetic angle-changing technique. These differential cross sections have been integrated to yield the elastic integral and momentum transfer cross sections at the above energies. These new results are compared with the most recent measurements and calculations of the respective cross sections in krypton. The dependence of the differential cross sections on atomic polarizability of the heavier rare gas atoms argon, krypton, and xenon has also been investigated over the electron energy range 5–30 eV and for forward, backward, and intermediate scattering angles.

I. INTRODUCTION

Experimental studies of electron scattering by the heavier rare-gas atoms in the low-energy region are particularly important from the point of view of developing adequate theoretical models for correlation-polarization interactions and relativistic effects. The krypton atom with its $4p^6$ closed outer shell is an atomic target whose properties may be expected to lie between those of argon and xenon. Its polarizability is higher and the relativistic effects are more evident than in argon and indeed several cases of electron scattering in argon have been described using a nonrelativistic approach. Similarly to argon and xenon, the differential cross sections (DCSs) for elastic electron scattering by krypton in the 5–10 eV region exhibit a distinct minimum close to 120° and a maximum at 180°. Furthermore, below 30° the DCSs increase with decreasing scattering angle. These features, together with the Ramsauer-Townsend minimum at 0.7 eV, make krypton an additional, sensitive test case for theoretical scattering models. Although the first measurements of elastic DCSs in krypton over a wide angular range, from 15° to 167.5°, were carried out in the early 1930s by Ramsauer and Kollath [1], they were performed with insufficient angular resolution to fully show the detailed angular behavior of the DCSs. Recent absolute DCSs data for krypton are scarce and cover narrower scattering angle ranges, typically up to or below 135°. Moreover, there are significant discrepancies between the existing experimental and theoretical determinations of the DCSs. The main purpose of the present work is to provide a set of DCSs for elastic scattering in krypton over an extended angular range in the low-energy regime. We present measurements of DCSs in krypton performed over scattering angle range from 30° to 180° and at incident electron energies of 5, 7.5, and 10 eV. To access angles over the whole backward scattering range, up to 180°, a magnetic angle changer [2] has been employed in these measurements. Absolute DCSs were obtained by application of the relative flow technique. The measurements are for elastic electron scattering in krypton up to 180°, for electron energies below 10 eV. In addition, we have integrated these DCSs to obtain the elastic integral and momentum transfer cross sections at the above energies.

Previously, absolute DCSs in krypton have been obtained by Williams and Crowe [3] in the energy range 20–400 eV and up to a scattering angle of 150°, Srivastava *et al.* [4] (3–100 eV, up to 135°), Weyhreter *et al.* [5] (0.05–2 eV, up to 100°), Danjo [6] (5–200 eV, up to 125°), and Milosavljević *et al.* [7] (20–260 eV, up to 110°–150° depending on the energy). Recently Cho *et al.* [8,9] used the magnetic angle-changing technique to measure the DCSs from 15° to 180° in the energy range 10–100 eV. Relative DCSs have been determined in the past by Webb [10], Lewis *et al.* [11], and Heindorff *et al.* [12]. Total cross sections in krypton were obtained for the first time by Ramsauer [13] in the early 1920s. More recently, total cross sections have been obtained in the following works that concentrated on the low-energy region: Dababneh *et al.* [14], Synapius *et al.* [15], Jost *et al.* [16], Subramanian and Kumar [17], Buckman and Lohmann [18], and Szmytkowski *et al.* [19]. For an extended list of references on the total cross-section measurements, the reader is directed to Ref. [19]. Elastic integral and momentum transfer cross sections in krypton have been previously determined by Srivastava *et al.* [4] and Danjo [6], after extrapolation of their measured DCSs down to 0° and up to 180°, and by Cho *et al.* [8] whose results required extrapolation only down to 0°. Momentum transfer cross sections have been obtained in electron-swarm experiments, which provide values of electron transport coefficients, by Frost and Phelps [20], Koizumi *et al.* [21], Hunter *et al.* [22], Suzuki *et al.* [23], and Schmidt *et al.* [24]. Preferred momentum transfer cross sections have been given recently by Buckman *et al.* [25].

A considerable number of theoretical calculations have been carried out for electron elastic scattering in krypton, using various approaches to take into account correlation-polarization and exchange interactions and relativistic effects. The R-matrix method has been applied by Fon *et al.* [26] and Bell *et al.* [27] in calculations that neglected relativistic effects. In these calculations the static dipole polarizability of the target atom was taken into account by coupling a ^1P pseudo-state (different for the two calculations) to the atomic ground state. The polarized-orbital method has been used by McEachran and Stauffer [28] within an adiabatic exchange approximation. This method included a dipole polarization potential and treated exchange exactly.

Mimnagh *et al.* [29] extended the polarized-orbital method presented in [28] in calculations which included dynamic distortion effects. More recently, McEachran and Stauffer [30] and Cho *et al.* [9] used the relativistic polarized-orbital method, which included static and dynamic polarization potentials and also a complex absorption potential to account for the loss of flux into open inelastic channels. Their calculations, improved agreement with experimental results in the intermediate and high-angular range, for the 20–100 eV energy range and proved the important role played by absorption. These works were further developed by Chen *et al.* [31] by development of a nonlocal, ab initio absorption potential that was applied to both electron and positron scattering. Gianturco and Rodriguez-Ruiz [32] used density-functional theory to describe the short-range interaction and the polarization adiabatic approach (up to octupole polarization term) to describe the long-range interaction in their nonrelativistic calculations. Also, density-functional theory has been applied by Haberland *et al.* [33] in a Kohn-Scham-type one-particle theory, which included an exchange-correlation potential, derived from model pair correlation functions. Sin Fai Lam [34] has calculated scattering phase shifts and integral cross sections. He applied a semirelativistic method and included a polarization potential using a procedure based on the Pople-Schofield approximation, while the direct relativistic effects were included by the second-order Dirac potential. Polarization-correlation effects have also been accounted for by the use of model potentials in a number of calculations. Yuan and Zhang [35] in their modified static-exchange calculations included correlation, distortion, and polarization effects by the parameter-free correlation-polarization potential of Padial and Norcross [36], while the exchange interaction was treated exactly. Sienkiewicz and Baylis [37] applied the continuum-state relativistic Dirac-Fock method using a model potential with two parameters to account for the dipole and quadrupole correlation-polarization interactions and treated exchange exactly. A model potential was also used in the calculations of Basu *et al.* [38]. O'Connell and Lane [39] proposed a nonadjustable model potential that includes exchange and correlation effects by a hybridization of local electron-gas theory and the long-range polarization.

II. EXPERIMENTAL

The present measurements were carried out at Manchester University using an electrostatic electron spectrometer equipped with a magnetic angle changer to detect electrons scattered in the backward direction. The spectrometer has been described in detail previously [40]. Briefly, it consists of an electron monochromator and an electron energy analyzer, which can be rotated in the angular range from –10° to 120° with respect to the direction of the incident electron beam. The construction of the monochromator is based on a hemispherical selector having a mean radius of 50 mm. Two triple-aperture lenses are employed to focus the incident electron beam onto the target gas beam. A three-element cylindrical lens is used to decelerate and focus scattered electrons from the target region onto the entrance aperture of a hemispherical electron analyzer (20-mm mean radius), which is followed by a channel electron multiplier. The incident electron beam current is monitored by a Faraday cup that can be moved to intercept the beam.

The incident beam current was typically 5 nA. The target gas beam is produced by a single capillary of internal diameter 0.3 mm and length 10 mm. The overall energy resolution of the present measurements was 80 meV. The incident electron energy was calibrated to within ±30 meV against the position of the 2^2S resonance in elastic scattering from helium.

The design and properties of the magnetic angle changer used in these measurements have been described in detail by Linert *et al.* [2]. The angle changer consists of two pairs of coaxial solenoids of conical geometry, which produce magnetic field that is localized at the interaction region. The electrons that are incident on the target gas beam and the electrons that are scattered from the beam are deflected by the magnetic field through a fixed angle [41]. This deflection shifts the backward scattered electrons to the entrance of the electron analyzer, which now can be placed at a position that does not collide with the electron monochromator. During the measurements, the scattered electron analyzer was placed at a fixed position of 110° with respect to the initial direction of the incident electron beam. Then the scattering angles in the range from 120° to 180° were selected by suitably adjusting the solenoid currents. The measurements in the scattering angle range from 30° to 110° were made without application of the angle changer. The angular scale of the present measurements was calibrated against the deep minimum in the elastic DCS of argon that occurs at 117.5° at 10 eV [42]. The total uncertainty in the angular scale is estimated to be ±2° and the angular resolution is estimated to be 4°.

The DCSs for elastic scattering in krypton were made absolute by application of the relative flow technique [43,44] and selecting helium as the reference gas. Intensities of scattered electrons in krypton and helium were measured at each scattering angle over the angular range from 30° to 180° at 10° intervals. The gas flow rates for both gases were determined from measurements of the rate of pressure increase in a fixed volume of the gas line. The ratios of scattering intensities in krypton to that in helium and the calculated cross sections of Nesbet [45] for helium were then used to determine absolute DCSs in krypton. The ratio of the driving pressures behind the beam-forming capillary in krypton with respect to helium was equal to 0.28 to fulfill the requirement of equal mean-free-path lengths in the capillary for both gases. The driving pressure for krypton was maintained below 15 Pa. During the measurements, both krypton and helium were continuously admitted to the vacuum chamber to obtain operational stability of the electron spectrometer. In this procedure, one gas was admitted directly to the scattering region through the capillary while the other was admitted to the main vacuum chamber through a side valve. Any background contributions to the scattering intensities were determined for each measurement by introducing both gases directly into the main chamber through side valves.

The statistical uncertainties in the measured DCSs arise from the statistical variations in the scattered electron intensities in krypton and helium, their relative flow rates, and the incident electron current, while the uncertainty in the theoretical elastic cross section of helium was taken to be 1%. At each scattering angle and incident electron energy a series of measurements was undertaken and the overall uncertainty in the measured absolute DCSs is estimated to be 15%.

TABLE I. Differential cross sections, in units of 10^{-20} m^2 sr^{-1}, for elastic electron scattering in krypton at incident energies of 5, 7.5, and 10 eV.

Scattering angle (deg)	Energy		
	5 eV	7.5 eV	10 eV
30	1.041	3.590	6.246
40	1.101	2.368	3.778
50	1.275	1.952	2.364
60	1.606	1.943	1.568
70	1.779	1.988	1.393
80	1.728	1.862	1.242
90	1.359	1.399	0.907
100	0.793	0.754	0.489
110	0.257	0.197	0.162
115	0.126	0.049	0.136
117	0.087	0.029	–
120	0.090	–	0.213
121	–	0.059	–
123	–	0.096	–
125	0.109	–	–
128	0.135	–	–
130	0.166	0.384	0.613
133.5	0.329	–	–
140	0.740	1.520	1.577
150	1.469	2.909	3.095
160	2.310	4.425	4.377
170	2.799	5.136	4.926
180	2.851	5.619	5.882

III. RESULTS AND DISCUSSION

A. Differential cross sections

The DCSs measured in this work for electron elastic scattering in krypton at the energies of 5, 7.5, and 10 eV are shown in Figs. 1, 2, and 3, respectively. These measurements cover the extended scattering angle range, 30°–180°. Available results of previous measurements [1,4,6,8] and theoretical calculations [26–28,34,37,46] are also shown for comparison. Numerical values of the present DCSs are listed in Table I.

At the energy of 5 eV (Fig. 1) the present DCS is in agreement with the experimental results of Danjo [6] in the scattering angle range up to 120° and with those of Srivastava *et al.* [4] up to 100°. Above 100° the DCS of Srivastava *et al.* is lower than the present results (by about 30% at 110°) and indicates a position for the minimum in the cross section that is at a lower scattering angle than is seen in the present work. Above 120°, both the measurements of Danjo and Srivastava *et al.* are higher than the present cross sections by a factor of two. The very early results of Ramsauer and Kollath [1] (at 4.6 eV) agree very well in the range of forward scattering, below 100°, with the more recent measurements. The best agreement between the theoretical calculations and the experimental DCSs is shown by the results of the R-matrix calculations of Bell *et al.* [27] and the relativistic calculations of Sienkiewicz and Baylis [37]. This is especially the case for the region of backward scattering, above 90°, where theory and experiment overlap. The relativistic calculations of Ref. [37] used a model potential to account for correlation-polarization
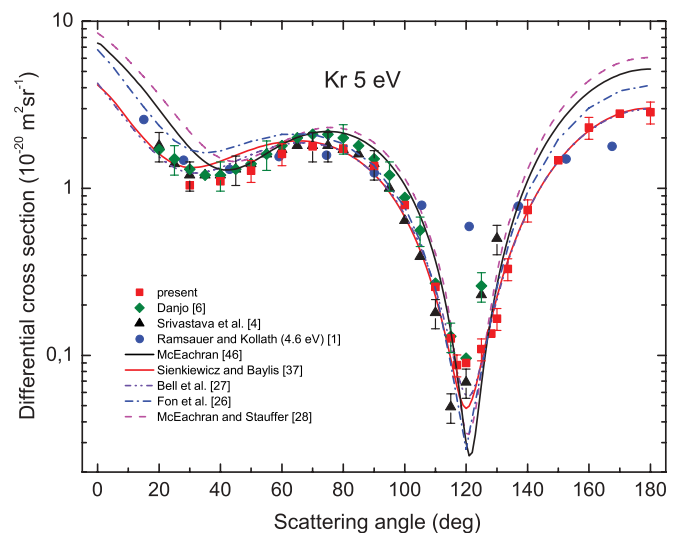

FIG. 1. (Color online) Differential cross sections for electron elastic scattering in krypton at the energy of 5 eV; squares show present results. In the figure are also shown the experimental results of Ramsauer and Kollath [1], Srivastava *et al.* [4], and Danjo [6] and the theoretical results of McEachran and Stauffer [28], Fon *et al.* [26], Bell *et al.* [27], Sienkiewicz and Baylis [37], and McEachran [46].

interactions and treated exchange exactly, whereas those of Ref. [27] used the method of coupling pseudo-states to account for the static dipole polarizability of the target atom. The results of the R-matrix calculations of Fon *et al.* [26] are in less good agreement with the experimental DCSs. They differ from the calculations of Bell *et al.* [27] in the configuration of the ^1P pseudo-state applied. The earlier polarized-orbital calculations of McEachran and Stauffer [28] gave results that significantly overestimated the DCSs above 130° and below 40°. Their more recent relativistic calculations [30,46] have brought slightly improved agreement with the experimental cross sections.

At the energy of 7.5 eV (Fig. 2) the present DCS agrees well with the results of Srivastava *et al.* [4] and Danjo [6] in the scattering angle range up to 100°. Above 100° both these cross sections again show a minimum in the angular dependence at a lower scattering angle (by about 4°) than the present measurements. Above the cross-section minimum, both results are higher than the present DCS by a factor of about 2. Again, the theoretical calculations of Sienkiewicz and Baylis [37] are in agreement with the present DCS although the positions of their predicted minimum in the cross section (close to 120°) lies slightly below our experimental value. A greater deviation from the experimental cross sections is found for the results of McEachran and Stauffer [28], however, their more recent relativistic calculations [30,46] gave a cross section that comes closer to the experimental results.

At the energy of 10 eV, which lies just above the first excitation threshold of the $5s[1^1/_2]°$ state of krypton at 9.915 eV, the present DCS (Fig. 3) is in very good accord over the whole angular range with the recent results of Cho *et al.* [8]. Those authors also employed the magnetic angle-changing technique, although their source for the localized magnetic field is of a different construction to that used in the present measurements. The DCS of Danjo [6] agrees with the present cross section and those of Ref. [8] up to 70°, but above 70°,
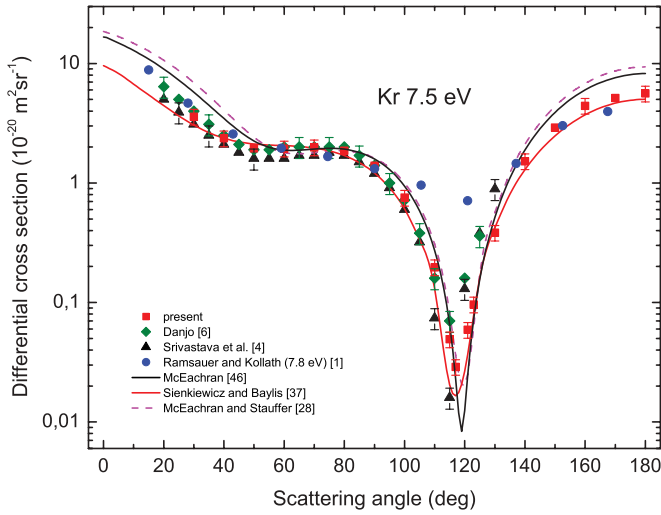
FIG. 2. (Color online) Differential cross sections for electron elastic scattering in krypton at the energy of 7.5 eV; squares show present results. In the figure are also shown the experimental results of Ramsauer and Kollath [1], Srivastava *et al.* [4], and Danjo [6] and the theoretical results of McEachran and Stauffer [28], Sienkiewicz and Baylis [37], and McEachran [46].

it starts to deviate and is higher than both measurements. The DCSs of Srivastava *et al.* [4] below 70° are systematically 20% lower than both measurements and show a deeper minimum near 107° again suggesting that their measurements most likely had higher angular resolution. Surprisingly good agreement is found between the early results of Ramsauer and Kollath [1] (of 10.6 eV) and the more recent measurements except over the region of the minimum in the cross section. Turning to a comparison with the theoretical calculations, it can be seen from Fig. 3 that more of the various theoretical approaches
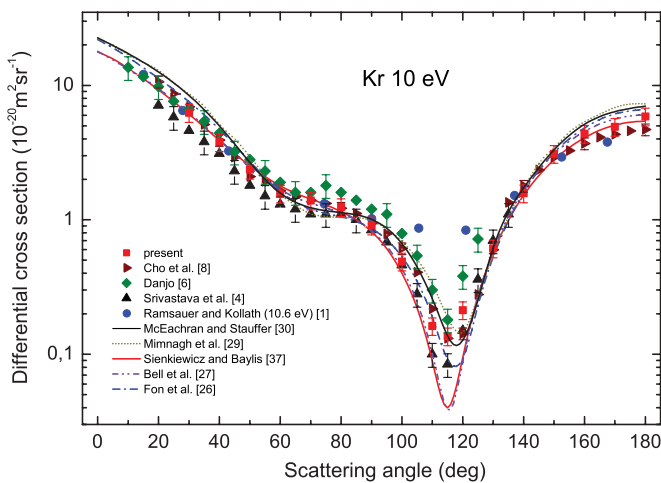

FIG. 3. (Color online) Differential cross sections for electron elastic scattering in krypton at the energy of 10 eV; squares show present results. In the figure are also shown the experimental results of Ramsauer and Kollath [1], Srivastava *et al.* [4], Danjo [6], and Cho *et al.* [8] and the theoretical results of Fon *et al.* [26], Bell *et al.* [27], Sienkiewicz and Baylis [37], Mimnagh *et al.* [29], and McEachran and Stauffer [30].

TABLE II. Integral cross section σ_t and momentum transfer cross section σ_m, in units of 10^{-20} m^2, for elastic electron scattering in krypton.

Energy (eV)	σ_t	σ_m
5	14.4	12.7
7.5	23.1	18.9
10	27.3	18.6

[26,27,37] give good overall agreement with the experimental cross sections than is the case at 7.5 and 5 eV. The earlier, extended polarized-orbital calculations of Mimnagh *et al.* [29] and the more recent relativistic polarized-orbital calculations of McEachran and Stauffer [30] give similar results, but show the lowest level of agreement with the measured DCSs for forward and backward scattering.

B. Integral and momentum transfer cross sections

We have determined the integral elastic (σ_t) and the momentum transfer (σ_m) cross sections for elastic scattering in krypton at electron energies of 5, 7.5, and 10 eV. Both cross sections were obtained by extrapolating the DCSs from 30° down to 0° and then integrating the DCSs over the complete angular range 0°–180°. In the extrapolation procedure for the 0°–30° range, we have taken the angular dependencies of the theoretical data of Bell *et al.* [27], which we normalized to our DCSs at 30°. The uncertainty in the integral and momentum transfer cross sections due to this extrapolation procedure is estimated to be less than 2% and 0.1%, respectively. We estimate that the associated uncertainties in the presented elastic integral and momentum transfer cross sections are 17% and 15%, respectively. Both cross sections are listed in Table II.

In Fig. 4 the integral cross sections obtained at 5, 7.5, and 10 eV are compared with cross sections determined from other previously measured DCSs [4,6,8], with available total cross sections [14–19] and with the results of theoretical calculations [26,27,29,30,32,34]. Very good agreement is found between the present integral cross sections and the experimental total cross sections, which usually have a higher degree of accuracy than DCSs. At 10 eV, the contribution of the excitation cross section of the first excited state $5s[1^1/_2]°$ of krypton at 9.915 eV to the total cross section is very small ($\sim$2%) and has been neglected. Above 5 eV the results of Danjo [6] overestimate the integral cross section whereas those of Srivastava *et al.* [4] largely underestimate it. These differences may, to some extent, arise from the extrapolation of their DCSs over the wide scattering angle range 130°–180°. With respect to the theoretical integral cross sections, again the results of Bell *et al.* [27] closely follow the experimental results.

The momentum transfer cross sections determined at 5, 7.5, and 10 eV are compared in Fig. 5 with those determined from previous DCS measurements [4,6,8], with results of swarm experiments [21–23], with theoretical cross sections [26,27,29,30,32,34] and with the preferred cross sections given by Buckman *et al.* [25] in the subvolume
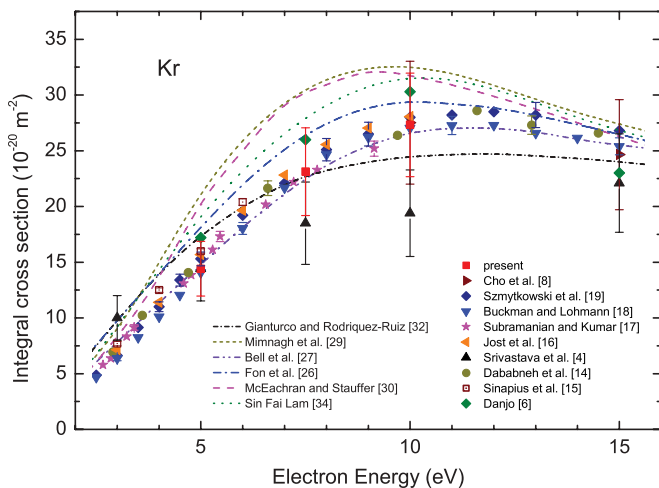
FIG. 4. (Color online) Integral cross sections for elastic electron scattering in krypton; squares show present results. In the figure are also shown the experimental results of Srivastava *et al.* [4], Danjo [6], and Cho *et al.* [8], the theoretical results of Fon *et al.* [26], Bell *et al.* [27], Mimnagh *et al.* [29], McEachran and Stauffer [30], and Gianturco and Rodriques-Ruiz [32], and the experimental total cross sections of Sinapius *et al.* [15], Dababneh *et al.* [14], Jost *et al.* [16], Subramanian and Kumar [17], Buckman and Lohmann [18], and Szmytkowski *et al.* [19].

"Interactions of Photons and Electrons with Atoms" of Landolt-Börstein. The present cross sections agree very well with those obtained from swarm experiments by Hunter *et al.* [22] and Suzuki *et al.* [23]. However, the integrated results of Srivastava *et al.* [4] and Danjo [6] deviate from the above determinations. We have found in the integration procedure that the 130°–180° angular range
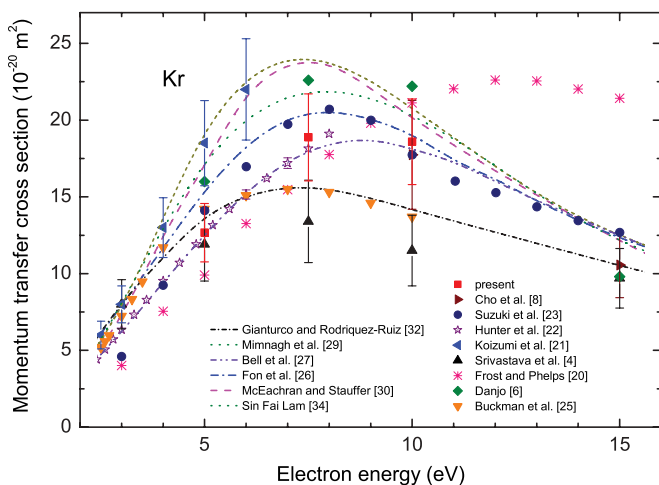

FIG. 5. (Color online) Momentum transfer cross sections in krypton: squares show present results. In the figure are also shown the experimental results of Srivastava *et al.* [4], Danjo [6], Cho *et al.* [8], Frost and Phelps [20], Koizumi *et al.* [21], Hunter *et al.* [22], and Suzuki *et al.* [23], the theoretical results of Fon *et al.* [26], Bell *et al.* [27], Mimnagh *et al.* [29], McEachran and Stauffer [30], and Gianturco and Rodriques-Ruis [32], and the preferred values of Buckman *et al.* [25].

gives a significant (40%–60%) contribution to the momentum transfer cross section, which therefore relies upon an accurate determination of the DCS in the backward scattering direction. It can also be seen that the preferred momentum transfer cross sections of Buckman *et al.* [25] tend to decrease above 7 eV, and at 10 eV are below the present value by about 30%. With respect to the theoretical results, the R-matrix calculations of Bell *et al.* [27], as expected, are in the best accord with the experimental cross sections.

C. Comparison of the differential cross sections of argon, krypton, and xenon

As noted above, the atoms of the heavier rare gases, argon, krypton, and xenon, are suitable targets to study the relative importance of polarization and correlation-polarization interactions in electron scattering and their adequate description. They are closed-shell atoms that differ in their polarizability, which increases with the number of atomic electrons. It is generally acknowledged that in the scattering of low-energy electrons, the dipole polarization interaction affects forward scattering whereas the non-adiabatic, free-bound electron-correlation effect shows up in backward scattering together with exchange interaction. To elucidate the contribution of the dipole polarization interaction, we compare in Fig. 6 the DCSs of the three atoms at fixed scattering angles of 30°, 80°, and 180° [Figs. 6(a), (b), and (c), respectively]. These angles correspond to the regions of forward, intermediate-angle, and backward scattering, respectively. The cross sections, taken from the present work and Refs. [8,9,47–51], are plotted as a function of atomic polarizability for several electron energies. The atomic polarizability represents here the strength of the long-range dipole polarization interaction. This long-range interaction merges with the short-range correlation-polarization interaction when the impinging electron moves closer to and starts to penetrate the target atom.

We find that at 30° (Fig. 6) the DCSs for 5 and 7.5 (7.9) eV increase strongly with increasing atomic polarizability. At 10 eV, the rate of increase begins to slow and appears to turn into a decrease at 30 eV. At 80° (Fig. 6), the DCSs for 5, 7.5, and 10 eV depend weakly or are independent of the atomic polarizability. For backward scattering at 180° [Fig. 6(c)], the DCS for 5 eV again increases strongly with polarizability; the DCS at 7.5 eV also increases, but less strongly than at 5, and at 10 eV appears to be slightly decreasing. Furthermore, the transition to a decreasing slope occurs at a lower energy than it does at 30°. It is seen from this comparison of the DCSs that the long-range dipole polarization interaction (as determined by the polarizability of the target) contributes significantly at 5–10 eV for 30° and 5–7.5 eV for 180°. A possible explanation for the observed weakening of the polarizability dependence of the DCSs with increasing energy is that the nonadiabatic effects (i.e., the increasing velocity of the incoming electron) lower the strength of the long-range polarization interaction and produce lower DCSs. At 30°, this effect begins at an energy above 20 eV, but at 180° it begins above 7.5 eV. Moreover, this effect appears to be greater in xenon than in argon. Clearly, systematic theoretical studies would be helpful to establish the contributions of the various electron-target interactions, including exchange, in this low-energy regime.
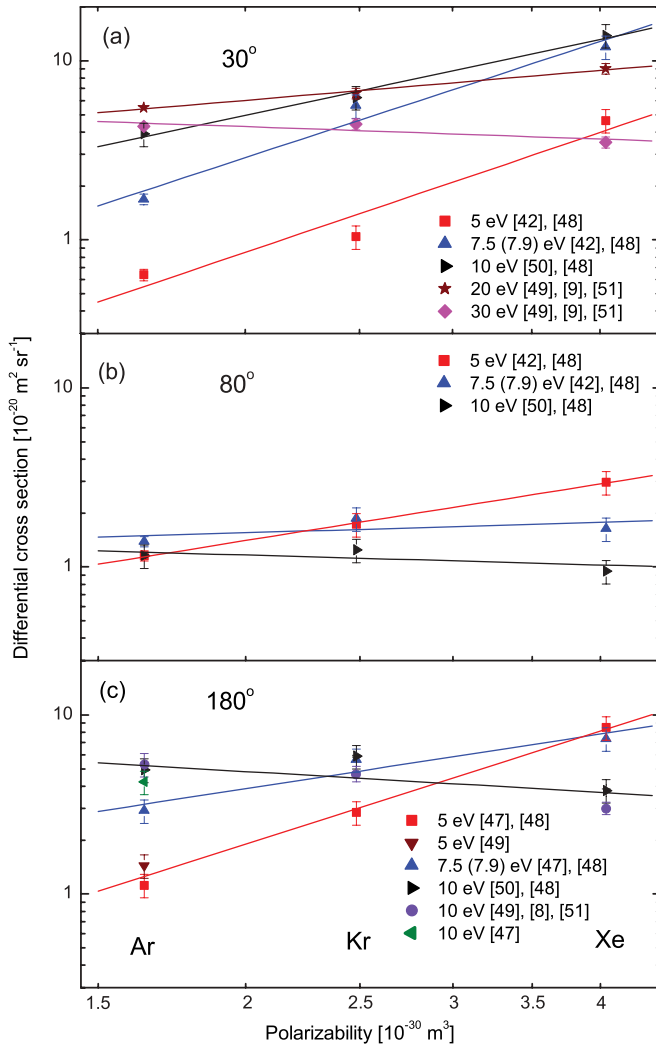
FIG. 6. (Color online) Differential cross sections of argon, krypton, and xenon plotted as a function of atomic polarizability over the electron energy range 5–30 eV at the scattering angles of: (a) 30°, (b) 80°, and (c) 180°. In the figures, apart from the present results for Kr, are shown results taken from the following Refs.: (a) for 5 and 7.5 (7.9) eV, Ar [42], Xe [48]; for 10 eV, Ar [50], Xe [48]; for 20 and 30 eV, Ar [49], Kr [9], Xe [51], (b) for 5 and 7.5 (7.9) eV, Ar [42], Xe [48]; for 10 eV, Ar [50], Xe [48], (c) for 5 eV, Ar [47,49], Xe [48]; for 7.5 (7.9) eV, Ar [47], Xe [48]; for 10 eV, Ar [47,49,50], Kr [8], Xe [48,51].

IV. CONCLUSIONS

We have measured DCSs for elastic electron scattering from krypton at energies of 5, 7.5, and 10 eV over the extended scattering angle range 30°–180°. Our measurements indicate that in this low-energy region, the theoretical calculations of Bell *et al.* [27] (R-matrix approach using pseudo-states) and Sienkiewicz and Baylis [37] (relativistic calculations applying model potential) show the best agreement with the experimental cross sections over the complete scattering angle range. On the other hand, the polarized-orbital calculations of McEachran and Stauffer [28,46] overestimate the DCSs in the forward and backward scattering regions. Interestingly, however, as seen from Ref. [48] and the present results, at 7.9 and 10 eV the polarized–orbital calculations are in better agreement with the measured cross sections in xenon than they are for krypton.

Integral elastic and momentum transfer cross sections have been obtained from the present DCSs by integration over the complete angular range 0°–180°. The present elastic integral cross section is in very good accord with the measured absolute total cross sections, whereas the momentum transfer cross section agrees with the results of the swarm experiments of Suzuki *et al.* [23] and Hunter *et al.* [22]. We conclude that the preferred momentum transfer cross section given in subvolume "Interactions of Photons and Electrons with Atoms" of Landolt-Börstein by Buckman *et al.* [25] is underestimated above 7 eV.

We have analyzed the DCSs of the three heavier rare gas atoms, argon, krypton, and xenon, as a function of their polarizabilities at the scattering angles of 30°, 80°, and 180° and electron energies in the range 5–30 eV. We find that, at lower energies 5 and 7.5 eV, the DCSs tend to increase strongly with increasing atomic polarizability, indicating significant contribution of long-range dipole polarization interaction. That dependence becomes weaker or disappears at higher energies, possibly as a result of nonadiabatic effects.

[1] C. Ramsauer and R. Kollath, Ann. Phys. Lpz. **12**, 837 (1932).
[2] I. Linert, G. C. King, and M. Zubek, J. Electron Spectrosc. Rel. Phenom. **134**, 1 (2003).
[3] J. F. Williams and A. Crowe, J. Phys. B **8**, 2233 (1975).
[4] S. K. Srivastava, H. Tanaka, A. Chutjian, and S. Trajmar, Phys. Rev. A **23**, 2156 (1981).
[5] M. Weyhreter, B. Barzick, A. Mann, and F. Linder, Z. Phys. D **7**, 333 (1988).
[6] A. Danjo, J. Phys. B **21**, 3759 (1988).
[7] A. R. Milosavljević, V. I. Kelemen, D. M. Filipović, S. M. Kazakov, V. Pejčev, D. Sević, and B. P. Marinković, J. Phys. B **38**, 2195 (2005).
[8] H. Cho, R. J. Gulley, and S. J. Buckman, J. Korean Phys. Soc. **42**, 71 (2003).
[9] H. Cho, R. P. McEachran, H. Tanaka, and S. J. Buckman, J. Phys. B **37**, 4639 (2004).
[10] G. M. Webb, Phys. Rev. **47**, 379 (1935).
[11] B. R. Lewis, I. E. McCarthy, P. J. O. Teubner, and E. Weigold, J. Phys. B **7**, 2549 (1974).
[12] T. Heindorff, J. Höfft, and P. Dabkiewicz, J. Phys. B **9**, 89 (1976).
[13] C. Ramsauer, Ann. Phys. **72**, 345 (1923).
[14] M. S. Dababneh, W. E. Kauppila, J. P. Downing, F. Laperriere, V. Pol, J. H. Smart, and T. S. Stein, Phys. Rev. A **22**, 1872 (1980).
[15] G. Sinapius, W. Raith, and W. G. Wilson, J. Phys. B **13**, 4079 (1980).

[16] K. Jost, P. G. F. Bisling, F. Eschen, M. Felsmann, and L. Walther, in *Proceedings of the 13th International Conference on the Physics of Electronic and Atomic Collisions, Berlin, 1983*, edited by J. Eichler (North-Holland, Amsterdam, 1983), p. 91.

[17] K. P. Subramanian and V. Kumar, J. Phys. B **20**, 5505 (1987).

[18] S. J. Buckman and B. Lohmann, J. Phys. B **20**, 5807 (1987).

[19] C. Szmytkowski, K. Maciąg, and G. Karwasz, Phys. Scr. **54**, 271 (1996).

[20] L. S. Frost and A. V. Phelps, Phys. Rev. **136**, A1538 (1964).

[21] T. Koizumi, E. Shirakawa, and I. Ogawa, J. Phys. B **19**, 2331 (1986).

[22] S. R. Hunter, J. G. Carter, and L. G. Christophorou, Phys. Rev. A **38**, 5539 (1988).

[23] M. Suzuki, T. Taniguchi, and H. Tagashira, J. Phys. D **22**, 1848 (1989).

[24] B. Schmidt, K. Berkhan, B. Götz, and M. Müller, Phys. Scr. **T53**, 30 (1994).

[25] S. J. Buckman, J. W. Cooper, M. T. Elford, M. Inokuti, Y. Itikawa, and H. Tawara, in *Landolt-Börstein, Photon and Electron Interaction with Atoms, Molecules and Ions, Group I*, edited by Y. Itikawa (Springer, Berlin, 2000), Vol. 17 A.

[26] W. C. Fon, K. A. Berrington, and A. Hibbert, J. Phys. B **17**, 3279 (1984).

[27] K. L. Bell, K. A. Berrington, and A. Hibbert, J. Phys. B **21**, 4205 (1988).

[28] R. P. McEachran and A. D. Stauffer, J. Phys. B **17**, 2507 (1984).

[29] D. J. R. Mimnagh, R. P. McEachran, and A. D. Stauffer, J. Phys. B **26**, 1727 (1993).

[30] R. P. McEachran and A. D. Stauffer, J. Phys. B **36**, 3977 (2003).

[31] S. Chen, R. P. McEachran, and A. D. Stauffer, J. Phys. B **41**, 025201 (2008).

[32] F. A. Gianturco and J. A. Rodriguez-Ruiz, Z. Phys. D **31**, 149 (1994).

[33] R. Haberland, L. Fritsche, and J. Noffke, Phys. Rev. A **33**, 2305 (1986).

[34] L. T. Sin Fai Lam, J. Phys. B **15**, 119 (1982).

[35] J. Yuan and Z. Zhang, J. Phys. B **22**, 2581 (1989).

[36] N. T. Padial and D. W. Norcross, Phys. Rev. A **29**, 1742 (1984).

[37] J. E. Sienkiewicz and W. E. Baylis, J. Phys. B **25**, 2081 (1992).

[38] D. Basu, S. K. Datta, P. Kahn, and A. S. Ghosh, Phys. Rev. A **35**, 5255 (1987).

[39] J. K. O'Connell and N. F. Lane, Phys. Rev. A **27**, 1893 (1983).

[40] I. Linert, G. C. King, and M. Zubek, J. Phys. B **37**, 4681 (2004).

[41] F. H. Read and J. M. Channing, Rev. Sci. Instrum. **67**, 2372 (1996).

[42] J. C. Gibson, R. J. Gulley, J. P. Sullivan, S. J. Buckman, V. Chan, and P. D. Burrow, J. Phys. B **29**, 3177 (1996).

[43] M. A. Khakoo and S. Trajmar, Phys. Rev. A **34**, 138 (1986).

[44] J. C. Nickel, C. Mott, I. Kanik, and D. C. McCollum, J. Phys. B **21**, 1867 (1988).

[45] R. K. Nesbet, Phys. Rev. A **20**, 58 (1979).

[46] R. P. McEachran (private communication).

[47] B. Mielewska, I. Linert, G. C. King, and M. Zubek, Phys. Rev. A **69**, 062716 (2004).

[48] I. Linert, B. Mielewska, G. C. King, and M. Zubek, Phys. Rev. A **76**, 032715 (2007).

[49] H. Cho and Y. S. Park, Phys. Soc. **55**, 459 (2009).

[50] I. Linert, G. C. King, and M. Zubek (to be published).

[51] H. Cho, R. P. McEachran, S. J. Buckman, D. M. Filipović, V. Pejceč, B. P. Marinković, H. Tanaka, A. D. Stauffer, and E. C. Jung, J. Phys. B **39**, 3781 (2006).